



## Analogue of Rashba pseudo-spin-orbit coupling in photonic lattices by gauge field engineering

Y. Plotnik,<sup>1</sup> M. A. Bandres,<sup>1</sup> S. Stützer,<sup>2</sup> Y. Lumer,<sup>1</sup> M. C. Rechtsman,<sup>1</sup> A. Szameit,<sup>2</sup> and M. Segev<sup>1</sup>

<sup>1</sup>*Physics Department, Technion – Israel Institute of Technology, Haifa 32000, Israel*

<sup>2</sup>*Institute of Applied Physics, Friedrich-Schiller-Universität, Max-Wien-Platz 1, 07743 Jena, Germany*

(Received 5 June 2015; revised manuscript received 20 May 2016; published 7 July 2016)

We present, theoretically and experimentally, the observation of the Rashba effect in photonic lattices, where the effect is brought about by an artificial gauge field, induced by the geometry of the system. In doing that, we demonstrate a particular form of coupling between pseudospin and momentum, resulting in spin-dependent shifts in the spectrum. Our system consists of two coupled, oppositely tilted waveguide arrays, where the evolution of an optical beam allows for probing the dynamics of the evolving wave packets, and the formation of spectral splitting. We show that the Rashba effect can be amplified or decreased through optical nonlinear effects, which correspond to mean-field interactions in various systems such as cold-atom lattices and exciton-polariton condensates.

DOI: [10.1103/PhysRevB.94.020301](https://doi.org/10.1103/PhysRevB.94.020301)

Engineering the gauge field of a physical system is a crucial step in the effort to control the behavior of waves. In the past few years, recent advances have demonstrated the ability to design and implement artificial gauge fields in a variety of physical systems, which have played a major role in demonstrating various fascinating phenomena in both photonic and cold-atoms settings [1–7]. In this Rapid Communication, we explore, theoretically and experimentally, a method to create artificial gauge fields. We implement this method for demonstrating the Rashba effect.

The Rashba effect describes the coupling between the spatial and spin degrees of freedom of electrons in a crystal, arising when a perpendicular electric field is applied to electrons restricted to move only in two dimensions. The Rashba term in the electron Hamiltonian appears as a result of the relativistic motion of the electrons, and is of the form

$$H_{\text{Rashba}} = (\vec{k} \times \vec{\sigma}) \cdot \hat{z} = k_x \sigma_y - k_y \sigma_x, \quad (1)$$

where  $\vec{k}$  is the momentum of the electron restricted to move in the  $x$ - $y$  plane, and  $\vec{\sigma}$  are the Pauli matrices [8,9]. When added to the Hamiltonian of free electrons ( $H_{\text{free}} = \frac{\hbar^2 k^2}{2m}$ ,  $m$  is the mass of the electron), the Rashba term removes the degeneracy in electron energy of opposite spins, shifting the band structure of an electron of a given spin in momentum space, while shifting the orthogonal spin in the opposite direction.

In the 1990s, the Rashba effect was suggested as a tool for manipulating the spin of electrons in spintronics [10], and realized a few years later in a semiconductor heterostructure, where the spin-orbit interaction was controlled by a gate voltage [11]. Since then, it has become a fundamental building block of spintronics [12]. In the context of ultracold-atom physics, spin-orbit coupling was demonstrated in a Bose-Einstein condensate by using Raman transitions induced by two external lasers in order to couple two electronic levels of rubidium atoms [4]. In such systems, the two levels of the rubidium atoms play the role of the “up” and “down” spin, and since the two levels are coupled by an external electromagnetic (EM) wave (the laser field), the velocity of the atoms causes a Doppler shift of the EM waves, changing the coupling and making it momentum dependent. Recently, a quantum wire exhibiting the Rashba effect was suggested as a platform for

realizing Majorana fermions, where the unique modes reside on the edges of the wire [13].

In photonics, it was suggested that the polarization of light can act as a spin degree of freedom for spin-orbit coupling [14]. The concept underlying the Rashba effect has inspired a series of experiments in plasmonics, where circularly polarized light was coupled to surface plasmon polaritons, on a metasurface with broken inversion symmetry [15–17]. These intriguing experiments show how opposite circular polarizations of light couple to plasmonic modes with opposite group velocity and Rashba-like band structures. While these pioneering experiments unequivocally demonstrated the Rashba effect in optics, such experiments, which rely on interaction with the metasurface, cannot serve as a platform to study the actual dynamic evolution of the “spin” in the system. Namely, plasmonic systems are inherently lossy, hence these photonic Rashba experiments were carried out through plasmons propagating for short range (tens of microns) on a surface, without the ability to observe the actual propagation dynamics in the system. Another theoretical suggestion was to use gyrotropic materials to achieve a Rashba effect in photonic crystals, but thus far this idea has not been studied in experiments [18].

Here, we propose and demonstrate an effective Rashba effect in photonic lattices, in a way that allows us to probe the evolution of the pseudospin. We achieve this through photonic gauge field engineering, which is an emerging field of photonics [1–3,6]. Our scheme is comprised of two one-dimensional (1D) waveguide arrays on top of each other, but with their propagation direction at some angle with respect to one another. The waveguides within each array are evanescently coupled, with each array forming a 1D photonic lattice, while maintaining the two inclined arrays coupled to each other. The inclination of the coupled lattices results in a pseudospin-dependent Rashba term in the Hamiltonian describing the evolution of the system, and the coupling between the arrays gives rise to a gap in the dispersion curves of the lattices. We experimentally probe the system by launching laser light into the arrays, and demonstrate that a simple Hamiltonian with a Rashba term describes the experimental measurements and simulations. Finally, we study the effects of nonlinearity (i.e., mean-field interactions) on the system, and show that introducing weak nonlinearity makes the effect highly dependent on initial conditions, either increasing or

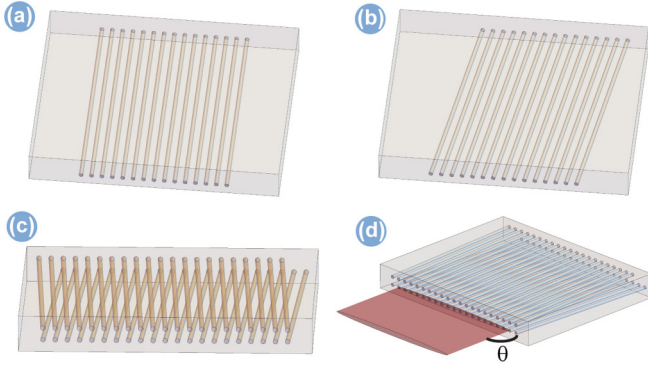


FIG. 1. Illustration of waveguide array structure. (a) A single 1D array of straight untilted waveguides. (b) A single array of tilted waveguides. (c) Two arrays, with the top one tilted to the left and the bottom one tilted to the right. (d) Illustration of the excitation method of the waveguide array. An elongated beam is launched at the input face of the sample. The angle of incidence,  $\theta$ , determines the transverse momentum  $k$  of the excitation.

decreasing the rate of spin oscillations, for symmetric or antisymmetric excitations of the system.

The evolution of monochromatic light traveling in a one-dimensional waveguide array with a low refractive index contrast [Fig. 1(a)] can be described by the paraxial wave equation,

$$i\partial_z\psi(\vec{r}) = -\frac{1}{2k_0}\nabla_{\perp}^2\psi(\vec{r}) - \frac{k_0}{n_0}\Delta n(\vec{r})\psi(\vec{r}), \quad (2)$$

where  $\psi$  is the envelope of the electric field,  $k_0$  is the wave number in the bulk material,  $n_0$  is the ambient refractive index,  $\nabla_{\perp}^2 = \partial_x^2 + \partial_y^2$ , and  $\Delta n(\vec{r})$  is the refractive index profile as a function of coordinate  $\vec{r}$ . This equation is mathematically identical to the Schrödinger equation describing the evolution of a single quantum particle, with two important differences: the  $z$  coordinate plays the role of time and  $-k_0\Delta n(\vec{r})/n_0$  plays the role of the potential. Hence, a waveguide with a locally higher refractive index is analogous to a potential well, and the propagation distance in the waveguide structure determines the total “time” of evolution we can experimentally observe in the system. When the waveguide array is periodic in  $x$ , one can apply Bloch’s theorem and write  $\psi(\vec{r}) = e^{ikx-i\beta z}u(x, y)$ , where  $u$  is periodic in  $x$ , and  $k$  is the transverse momentum. When the light is tightly confined to the waveguides and the coupling between waveguides is evanescent (tunneling), we can describe the dynamics of  $\psi$  in the waveguide array using a tight-binding model. If only nearest-neighbor coupling is taken into account, the equation describing the evolution of light in the waveguide array is given by

$$i\partial_z\psi_n = t\psi_{n-1} + t\psi_{n+1},$$

where  $\psi_n$  is the amplitude at waveguide number  $n$ , and  $t$  is the coupling strength between neighboring waveguides (a negative number) [19]. When we substitute the Bloch solution,  $\psi_n = e^{ikan-i\beta z}$ , where  $a$  is the lattice constant (distance between adjacent waveguides) and  $\beta$  is the propagation constant, we find the simple dispersion relation  $\beta = 2t\cos(ka)$ . Thus far we have simply explained the analogy between a 1D waveguide array and a periodic potential in quantum mechanics, and

how it can be described by a tight-binding model. This analogy has given rise to the observation of a plethora of phenomena predicted in solid-state physics, ranging from Bloch oscillations [20,21], Shockley edge states [22], and Zener tunneling [23] to more complex phenomena such as Anderson localization [24] and, more recently, photonic topological insulators [1]. Importantly, in our scheme, the waveguide arrays are tilted with respect to one another. When such a waveguide array is tilted, the waveguides are no longer parallel to the  $z$  axis, but instead have a slight angle in the  $x$  direction. In this case, the refractive index profile can be written as  $\Delta n(x - \eta z, y)$ , where  $\eta$  gives the tilt of the waveguides [Fig. 1(b)]. We now make a coordinate transformation to the reference frame moving with the waveguides  $x, y, z \rightarrow x', y, z$ , where  $x' = x - \eta z$ , and Eq. (2) becomes

$$i\partial_z\phi(\vec{r}') = \frac{1}{2k_0}(i\vec{\nabla}_{\perp} + \hat{x}\eta k_0)^2\phi(\vec{r}') - \frac{k_0}{n_0}\Delta n'(\vec{r}')\phi(\vec{r}') - \frac{1}{2}k_0\eta^2\phi(\vec{r}'), \quad (3)$$

giving us a vector potential of the form  $\vec{A} = \hat{x}\eta k_0$ , and a constant bias to the refractive index of magnitude  $\frac{1}{2}n_0\eta^2$ . Now, when writing the tight-binding model, the vector potential gives us an additional phase at the coupling (the Peierls substitution) yielding a new tight-binding equation,

$$i\partial_z\phi_n = te^{ik_0\eta a}\phi_{n-1} + te^{-ik_0\eta a}\phi_{n+1}, \quad (4)$$

with the shifted dispersion relation  $\beta' = 2t\cos(ka - k_0\eta a)$ . This means that our Bloch continuum solution is given by  $\psi(\vec{r}) = e^{ikx'-i\beta'z}u(x', y) = e^{ikx-i(\beta'+k\eta)z}u(x - \eta z, y)$ , where we made the substitution  $x' = x - \eta z$ . We thus get  $\beta$  in the fixed frame of reference,

$$\beta = \beta' + \eta k = 2t\cos(ka - k_0\eta a) + \eta k. \quad (5)$$

Notice that tilting the waveguide arrays has two effects: it introduces a shift in the band structure in momentum space and it adds a term linear with  $k$ . While the second effect clearly gives us a Rashba term, the first one is more reminiscent of the Rashba effect for a free electron, and when examined only in the vicinity of  $k = 0$ , it gives rise to a Rashba term with a sign opposite to that of the second term.

Now that we have a mechanism for obtaining a  $k$ -dependent term for the evolution of light in a titled waveguide array, we can construct a structure composed of two arrays: one tilted in the positive direction and one tilted in the negative direction, with one above the other as illustrated in Fig. 1(c). This results in a Hamiltonian of the form

$$H_k = \begin{pmatrix} 2t\cos(ka - \eta k_0 a) + \eta k & 0 \\ 0 & 2t\cos(ka + \eta k_0 a) - \eta k \end{pmatrix}, \quad (6)$$

which describes the band structure illustrated in Fig. 2(a). It is important to note that when we consider a single tilted array, the artificial gauge field is trivial and can be gauged out because it amounts to nothing more than a change of reference frame. However, when dealing with two arrays with different tilt angles, the gauge field becomes space dependent and nontrivial, i.e., there is no reference frame where both arrays are not tilted. Now, writing the Hamiltonian [Eq. (6)] in

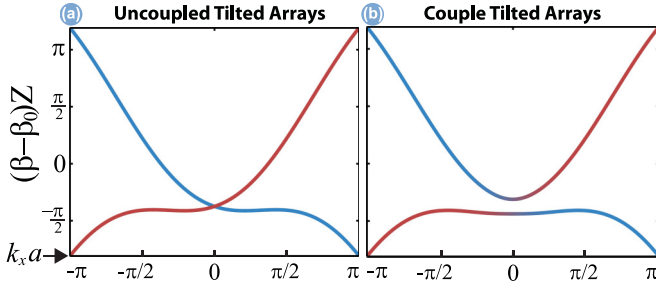


FIG. 2. (a) Calculated band structure of two tilted uncoupled waveguide arrays. The band structures of the top (red) and bottom (blue) waveguide arrays are shifted and tilted in opposite directions. (b) The band structure when the two arrays are coupled: a gap opens at  $k = 0$ , and each band starts at one array and switches to the other at the  $k = 0$  point (highlighted here by the gradual switching between the colors at  $k = 0$ ).

the basis given by

$$|\phi_1\rangle = \frac{1}{\sqrt{2}} \begin{pmatrix} 1 \\ i \end{pmatrix} \quad |\phi_2\rangle = \frac{1}{\sqrt{2}} \begin{pmatrix} 1 \\ -i \end{pmatrix}, \quad (7)$$

the Hamiltonian becomes

$$\begin{aligned} \tilde{H}(k) &= \begin{pmatrix} 2t\cos(ka)\cos(\eta k_0 a) & 2t\sin(ka)\sin(\eta k_0 a) + \eta k \\ 2t\sin(ka)\sin(\eta k_0 a) + \eta k & 2t\cos(ka)\cos(\eta k_0 a) \end{pmatrix}. \end{aligned} \quad (8)$$

For  $ka \ll \pi$ , we find that the Hamiltonian takes the form of a Rashba Hamiltonian along one dimension,

$$\tilde{H}_k \simeq -\frac{1}{2}a^2\cos(k_0\eta a)Ik^2 + [\sin(\eta k_0 a)2at + \eta]\sigma_x k,$$

where  $\sigma_x$  is the  $x$  Pauli matrix. This indeed shows that our system is an exemplary candidate for probing the Rashba effect in optics, including its evolution dynamics. Importantly, in this kind of setting, the strength of the Rashba term can be tuned by modifying the tilt of the arrays, the distance between sites, and/or the coupling between them. In our experimental setting, the Rashba term is dominated by  $\eta$  ( $at \ll \eta$ ) and the coupling within the array plays a minor role in determining the band structure, as seen in Fig. 2(a). Additionally, we bring the arrays close together so that light can couple from one array to

the other. This allows the phase of the optical field to have a measurable effect: the phase controls the directionality of the flow of light from one array to the other, as explained later. The coupling thus alters the band structure: it opens a gap at the crossing of the two bands at  $k = 0$ , as illustrated in Fig. 2(b).

In our experiments, we use waveguide arrays directly written into fused silica glass samples [25]. Each waveguide supports only one guided mode at the experimental wavelength of 633 nm, and the waveguides are separated from one another in the horizontal direction by  $20 \mu\text{m}$  within each array. The two arrays are separated in the vertical direction by  $28 \mu\text{m}$  and the tilt of each array is  $\eta = 2 \frac{\mu\text{m}}{\text{mm}}$ . We launch light into the waveguide arrays from the input facet, as illustrated in Fig. 1(d), and measure its intensity after it has evolved for a certain distance in the array. We shape the incoming beam to be broad in the  $x$  direction, so that it couples strongly to a well-defined Bloch mode of the array [Fig. 1(d)]. By changing the input angle of the incoming beam, we control the Bloch wavenumber  $k$  of the mode into which the beam couples. We emphasize again here that the spatial degree of freedom is the  $x$  position within a given array, and the pseudospin degree of freedom represents within which array (top or bottom) the light resides (the relative occupation of the top and bottom arrays).

As the light is propagating in the system, it couples from one array to the other. This can be seen in the experimental results shown in Fig. 3(c) [Fig. 3(f)] where light launched solely into the top [bottom] array couples to the bottom [top] array. The coupling is the strongest when the input angle corresponds to  $k \simeq 0$ , where the bands of the two arrays cross each other [Fig. 2(a)] and phase matching is achieved. This effect can also be seen in full continuum simulations of the paraxial equation, as shown in Fig. 3(b). What we also see in the continuum simulations is that for large  $k$ , there is strong attenuation in the evolution process. This happens because the refractive index (potential) is  $z$  dependent (time dependent) since each array is tilted relative to the other. This inevitably causes some  $k$ -dependent coupling to continuum modes. The further away  $k$  is from the axis of the tilted array, the more it couples to continuum modes, which is manifested as loss in the system. We may add this loss mechanism to our tight-binding model phenomenologically,

$$H_k = \begin{pmatrix} 2t\cos(ka - \eta k_0 a) + \eta k - i\gamma(ka - \eta k_0 a)^2 & t_2^{\text{bottom} \rightarrow \text{top}}(k) \\ t_2^{\text{top} \rightarrow \text{bottom}}(k) & 2t\cos(ka + \eta k_0 a) - \eta k - i\gamma(ka + \eta k_0 a)^2 \end{pmatrix}, \quad (9)$$

where  $\gamma$  is the loss rate, and  $t_2(k)$  is the coupling between the two arrays (see further details in the Supplemental Material [26]). This tight-binding model is corroborated using a method that we developed for calculating band structures of Floquet continuum Hamiltonians. This method and its comparison to the tight-binding model is also elaborated in the Supplemental Material [26].

We simulate the propagation in this system numerically [Fig. 3(a)] with this Hamiltonian [Eq. (9)] and find that the

results coincide with full continuum simulations [Fig. 3(b)]. Henceforth, all of our experiments and simulations are given for a propagation distance of 5 cm in our system, where the parameters are chosen such that at least one full power oscillation (between the waveguide arrays) can be observed.

We repeat the experiment multiple times for different input angles and plot the power at the output facet as a function of the transverse momentum  $k$ ; see Fig. 3(c). Next, we redo the experiment, only now we launch the beam into the bottom

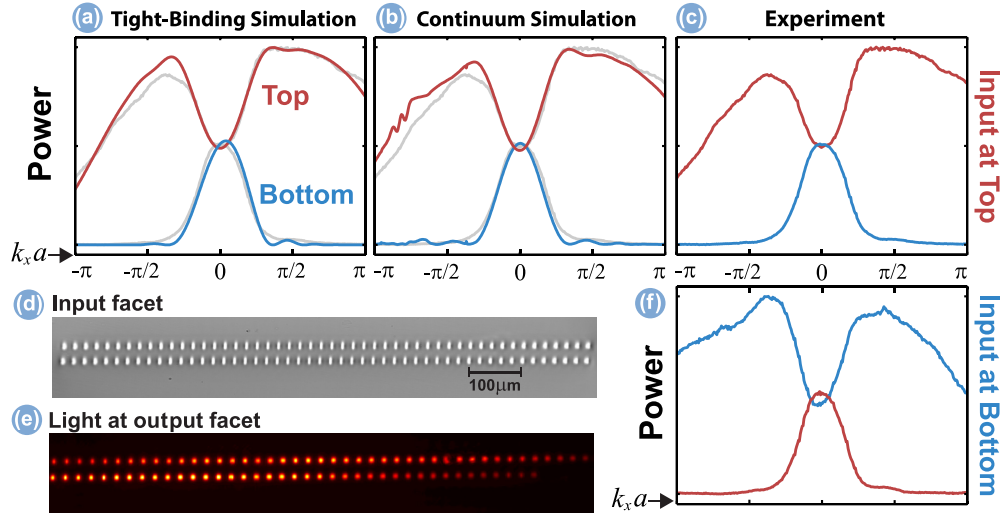


FIG. 3. Experimental results and simulations showing the optical intensity at the output face as a function of  $k$  at the top array (red) and the bottom array (blue). The light gray lines in (a) and (b) depict the experimental measurements for comparison. (a) Simulation using a simplified tight-binding model [Eq. (9)] with  $k$ -dependent loss. (b) Simulation using a continuum numerical propagator of the paraxial equation. (c) Experimental results when the beam is launched into the top array, as simulations in (a) and (b). (d) Microscope image of the input facet of the photonic lattice. (e) Example of typical experimental measurement of the light in the two arrays, observed at the output facet. (f) Experimental results when the beam is launched into the bottom array.

array, which is tilted in the opposite direction [Fig. 3(f)]. In both experiments, we observe a similar effect: light couples from one array to the other maximally around  $ka = 0$ . This happens because at this point the bands of the two arrays cross, and the phase matching between the two arrays allows for resonant coupling. Far from  $ka = 0$ , the two arrays are phase mismatched and thus the coupling is ineffective and no light is transferred between the arrays. This is in full agreement with our tight-binding Rashba model [Fig. 3(a)].

Next, we launch a broad beam (making the excitation correspond to a single Bloch mode, with a given value of  $k$ ) into both arrays. We do this for the two orthogonal pseudospin configurations: in one configuration we launch a symmetric beam, i.e., the elongated beam launched into both arrays has the same initial phase; in the other configuration we launch an antisymmetric beam, i.e., the initial phase in the top array is opposite to the initial phase at the bottom array. With these initial conditions, we observe, in experiments as well as in simulations, that light is transferred in an oscillatory manner between the top and bottom arrays, as a function of the transverse momentum  $k$  (Fig. 4).

While analyzing the dynamics of the occupations of the two arrays, we recall that the coupling between them acts as a directional coupler: when the phase difference between the two arrays ( $\Delta\Phi = \Phi_{\text{top}} - \Phi_{\text{bottom}}$ ) is in the range  $(-\pi, 0)$ , the power flows from the top array to the bottom array, reaching a maximum flow at  $-\pi/2$ , and if  $\Delta\Phi$  is in the  $(0, \pi)$  range, the power flows from the bottom array to the top one. This dynamics is identical to the dynamics in the electron spin system [9]. At  $k = 0$ , we see that the occupations at the output facets of both arrays remain equal for both symmetric and antisymmetric excitations, since the phase in the two arrays remains equal. Consider first the regime of  $k > 0$ . As we start at  $k = 0$  and increase  $k$ , we see that in the symmetric case, power flows from the top array to the bottom array. This is

because the bottom array accumulates phase faster than the top array, resulting in  $\Delta\Phi \in (-\pi, 0)$ , giving rise to power flow from top to bottom. In the antisymmetric case, since the two arrays begin with a relative phase of  $\pi$  from one another, as the bottom array acquires phase faster, it goes into the region of  $\Delta\Phi \in (0, \pi)$ , creating flow of power from bottom to top. This can also be described as a part of a beating (modal interference) phenomenon: since the mode of the bottom array

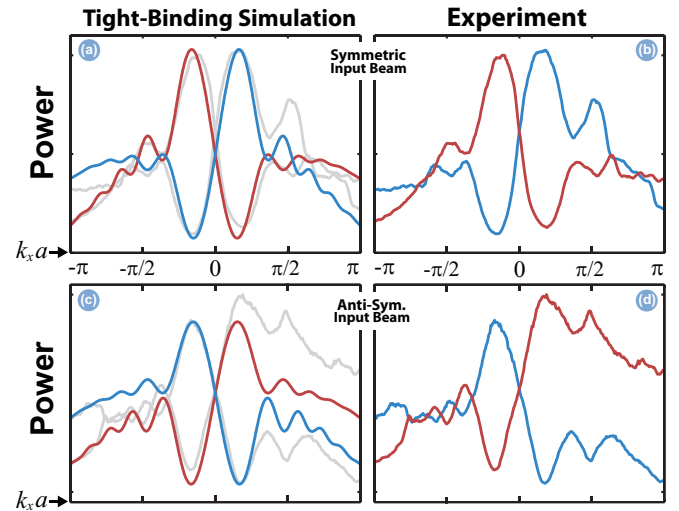


FIG. 4. (a), (c) Simulation showing the corresponding cases using the simple tight-binding model, for (a) symmetrical excitation and (c) antisymmetrical excitation. The light gray lines in (a) and (c) depict the experimental results for comparison. (b), (d) Experimental results showing the power at the output face of the top (red) and bottom (blue) arrays as a function of  $k$ . (b) The beam is launched into both arrays symmetrically (same phase). (d) The beam is launched into both arrays antisymmetrically (opposite phase).

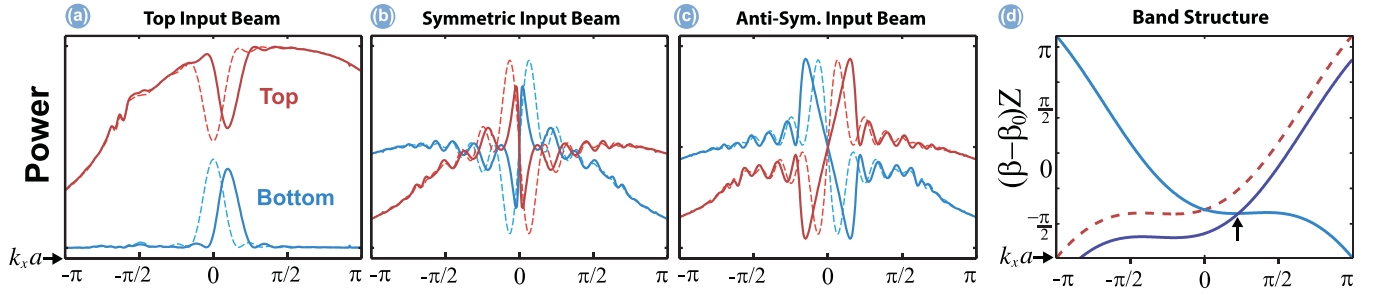


FIG. 5. Nonlinear continuum simulation results with  $\eta = 4 \frac{\mu\text{m}}{\text{mm}}$ . The light red and light blue dashed lines present the power at the top and bottom arrays (respectively) in the *linear* case. The red and blue solid lines present the power at the top and bottom arrays (respectively) in the *nonlinear* case. (a) The results when the system is excited at the top array. The point of maximal transmission from the top array to the bottom array has moved from  $k = 0$  to higher  $k$  values. (b) Symmetric excitation: the range of the oscillations becomes narrower due to accelerated beating between the band populations, as a consequence of the nonlinearity. (c) Antisymmetric excitation: the range of the oscillations becomes wider because of the nonlinearity. (d) Shifted band structure of the top array (purple solid line) as a result of the nonlinearity when only the top array is excited. As a consequence of the shift, the crossing point of the two bands, where light is transferred resonantly, has moved (arrow) to a higher value of  $k$ .

has a larger propagation constant than the mode of the top array for positive  $k$ , there are power oscillations between the arrays. When we excite the arrays symmetrically, we initialize the modes at a point where power starts flowing from top to bottom, and when we excite them antisymmetrically, we initialize it at a point where power starts flowing from the bottom to the top. As we go to even higher  $k$  values, we see oscillations in the power flow. This is caused by the fact that the difference in propagation constants becomes large, thus the beating rate increases and we see that power goes back and forth between the arrays. At high  $k$  values, the amplitude of power oscillations is attenuated because of phase mismatch and because most of the power is lost, until eventually the oscillations become insignificant. At negative  $k$  values, we see exactly the same effect, but the roles are now switched between the top and bottom arrays.

This realization of the Rashba effect in an optical setting allows for observing the evolution dynamics in experiments and suggests several new directions for study. The most immediate one is how does the Rashba system behave under nonlinearity? This question is directly relevant to cold-atoms system, where the optical self-focusing (defocusing) nonlinearity is equivalent to attractive (repulsive) mean-field interactions, and the potential landscape is induced by optical lattices. Here, we will consider the simplest kind of optical nonlinearity—the optical Kerr effect, where the optical field induces a refractive index change proportional to the light intensity. This kind of nonlinearity is modeled by the Gross-Pitaevskii equation and enters the paraxial equation [Eq. (1)] via the refractive index,

$$i\partial_z \psi(\vec{r}) = -\frac{1}{2k_0} \nabla_{\perp}^2 \psi(\vec{r}) - \frac{k_0}{n_0} [\Delta n(\vec{r}) + n_2 |\psi(\vec{r})|^2] \psi(\vec{r}). \quad (10)$$

We study the system through a full continuum simulation of Eq. (10). Even when taking into account relatively small refractive index changes of the order of  $10^{-5}$ , we find several intriguing results that can be explained in full by examining

the effect of the nonlinear index change on the band structure in Fig. 1(a).

First, let us consider the case where we excite only one array. In this case, the nonlinearity causes a shift of the  $k$  value for which power is maximally transferred from the excited array to the other array, as demonstrated in Fig. 5(a). The reason for this effect is that light launched into the top array causes its refractive index to increase, moving downwards its corresponding band due to the nonlinear effect [Fig. 5(d)]. This moves the crossing point of the two bands to a higher  $k$ , thus the resonant transfer of light between the two arrays occurs for a higher  $k$ . Next, consider the case where we excite both arrays. When we excite the arrays symmetrically, the occupation curve is squeezed towards  $k = 0$  [Fig. 5(b)]. This is because when light is initially transferred from one array to the other, the effective refractive index of the array into which the light was transferred increases (due to the nonlinear effect), thus light in this array accumulates phase faster [27]. This increases the rate at which light is transferred from one array to the other, and the whole process is accelerated. The same happens when light is transferred back after the initial oscillation, only now the index change slows down the process. Since what we see at the output facet close to  $k = 0$  is mostly a result of the initial beat (the first oscillation), we observe an accelerated power exchange process and thus the occupation picture is squeezed [Fig. 5(b)]. The reverse effect happens when we excite the arrays antisymmetrically. As light is transferred from one array to the other, the nonlinear refractive index change slows down the rate of accumulation of relative phase and thus the occupation picture is broadened [Fig. 5(c)]. It should be noted that the simulation results displayed in Fig. 5 are calculated with  $\eta = 4 \frac{\mu\text{m}}{\text{mm}}$ , resulting in oscillations in the linear case which are faster than in Fig. 4 where  $\eta = 2 \frac{\mu\text{m}}{\text{mm}}$ . We show the effect of nonlinearity for this choice of  $\eta$ , since it is more pronounced than in the  $\eta = 2 \frac{\mu\text{m}}{\text{mm}}$  because of a larger Rashba term in the Hamiltonian.

To conclude, we proposed and experimentally demonstrated an optical system that displays the Rashba effect. This system allows for monitoring the evolution of the

pseudospin using a simple optical setting of two countertilted waveguide arrays. We have shown the pseudospin evolution for several different initial conditions and analyzed the resulting output. We have calculated the effect of optical nonlinearity on the system, and have shown that it highly depends on initial conditions. This system demonstrates two artificial gauge field mechanisms, one adds a term linear in  $k$  to the Hamiltonian and the other adds a vector potential which shifts the band structure in momentum space. In the system demonstrated here, the first mechanism is dominant due to weak couplings between sites in the lattice. This raises the following questions: How would the system behave under strong coupling, where the artificial vector potential dominates the dynamics in the system? Can we mimic an artificial magnetic field by having multiple arrays with increasing tilts stacked one above the other? What other interesting effect can be achieved with these gauge fields? Can this mechanism be realized in a system of cold fermions? In such a system, can this scheme be a platform for observing the long-sought Majorana fermions? Finally, with the recent pioneering work on quantum random walk in exactly this

kind of system (waveguide arrays) [28–32], the experiments demonstrated here make it possible to explore the Rashba effect in the single-photon limit, where fundamental questions on quantum correlations can be addressed in experiments, and the evolution of entangled states in the Rashba system can be explored in the laboratory.

This research was supported by the German-Israeli DIP program, the Transformative Science Program of the Binational USA Israel Science Foundation (BSF) and by the Israeli ICORE Excellence Center “Circle of Light.” The research leading to these results has received funding from the European Union’s—Seventh Framework Programme (FP7/2007-2013) under Grant Agreement No. 629114 MC—Structured Light. M.C.R. acknowledges the support of the National Science Foundation under Grant No. ECCS-1509546. A.S. gratefully acknowledges financial support from the Deutsche Forschungsgemeinschaft (Grants No. SZ 276/7-1, No. SZ 276/9-1, No. BL 574/13-1, and No. GRK 2101/1) and the German Ministry for Science and Education (Grant No. 03Z1HN31).

- 
- [1] M. C. Rechtsman, J. M. Zeuner, Y. Plotnik, Y. Lumer, D. Podolsky, F. Dreisow, S. Nolte, M. Segev, and A. Szameit, *Nature (London)* **496**, 196 (2013).
- [2] M. C. Rechtsman, J. M. Zeuner, A. Tünnermann, S. Nolte, M. Segev, and A. Szameit, *Nat. Photon.* **7**, 153 (2012).
- [3] M. Hafezi, S. Mittal, J. Fan, A. Migdall, and J. M. Taylor, *Nat. Photon.* **7**, 1001 (2013).
- [4] Y.-J. Lin, K. Jiménez-García, and I. B. Spielman, *Nature (London)* **471**, 83 (2011).
- [5] G. Jotzu, M. Messer, R. Desbuquois, M. Lebrat, T. Uehlinger, D. Greif, and T. Esslinger, *Nature (London)* **515**, 237 (2014).
- [6] K. Fang, Z. Yu, and S. Fan, *Nat. Photon.* **6**, 782 (2012).
- [7] M. Aidelsburger, M. Lohse, C. Schweizer, M. Atala, J. T. Barreiro, S. Nascimbène, N. R. Cooper, I. Bloch, and N. Goldman, *Nat. Phys.* **11**, 162 (2015).
- [8] G. Dresselhaus, *Phys. Rev.* **100**, 580 (1955).
- [9] E. Rashba, *Sov. Phys.-Solid State* **2**, 1109 (1960).
- [10] S. Datta and B. Das, *Appl. Phys. Lett.* **56**, 665 (1990).
- [11] J. Nitta, T. Akazaki, H. Takayanagi, and T. Enoki, *Phys. Rev. Lett.* **78**, 1335 (1997).
- [12] I. Žutić, J. Fabian, and S. Das Sarma, *Rev. Mod. Phys.* **76**, 323 (2004).
- [13] J. Alicea, Y. Oreg, G. Refael, F. von Oppen, and M. P. A. Fisher, *Nat. Phys.* **7**, 412 (2011).
- [14] V. S. Liberman and B. Y. Zel’dovich, *Phys. Rev. A* **46**, 5199 (1992).
- [15] K. Frischwasser, I. Yulevich, V. Kleiner, and E. Hasman, *Opt. Express* **19**, 23475 (2011).
- [16] N. Shitrit, I. Yulevich, V. Kleiner, and E. Hasman, *Appl. Phys. Lett.* **103**, 211114 (2013).
- [17] N. Dahan, Y. Gorodetski, K. Frischwasser, V. Kleiner, and E. Hasman, *Phys. Rev. Lett.* **105**, 136402 (2010); N. Shitrit, I. Yulevich, E. Maguid, D. Ozeri, D. Veksler, V. Kleiner, and E. Hasman, *Science* **340**, 724 (2013).
- [18] V. Yannopoulos, *Phys. Rev. B* **83**, 113101 (2011).
- [19] F. Lederer, G. I. Stegeman, D. N. Christodoulides, G. Assanto, M. Segev, and Y. Silberberg, *Phys. Rep.* **463**, 1 (2008).
- [20] R. Morandotti, U. Peschel, J. Aitchison, H. Eisenberg, and Y. Silberberg, *Phys. Rev. Lett.* **83**, 4756 (1999).
- [21] T. Pertsch, P. Dannberg, W. Elflein, A. Bräuer, and F. Lederer, *Phys. Rev. Lett.* **83**, 4752 (1999).
- [22] N. Malkova, I. Hromada, X. Wang, G. Bryant, and Z. Chen, *Opt. Lett.* **34**, 1633 (2009).
- [23] H. Trompeter, T. Pertsch, F. Lederer, D. Michaelis, U. Streppel, A. Bräuer, and U. Peschel, *Phys. Rev. Lett.* **96**, 023901 (2006).
- [24] T. Schwartz, G. Bartal, S. Fishman, and M. Segev, *Nature (London)* **446**, 52 (2007).
- [25] A. Szameit and S. Nolte, *J. Phys. B: At. Mol. Opt. Phys.* **43**, 163001 (2010).
- [26] See Supplemental Material at <http://link.aps.org/supplemental/10.1103/PhysRevB.94.020301> for a detailed deduction of a tight binding model for coupled tilted waveguide arrays, and a method for the calculating the Floquet band structure and quasieigenmodes for a continuous time periodic model.
- [27] In principle, this nonlinear change in the refractive index unbalances the waveguides in terms of phase matching. However, this will have significant impact only after large propagation distances or high values of  $k$ .
- [28] H. B. Perets, Y. Lahini, F. Pozzi, M. Sorel, R. Morandotti, and Y. Silberberg, *Phys. Rev. Lett.* **100**, 170506 (2008).
- [29] Y. Bromberg, Y. Lahini, R. Morandotti, and Y. Silberberg, *Phys. Rev. Lett.* **102**, 253904 (2009).
- [30] I. Afek, O. Ambar, and Y. Silberberg, *Science* **328**, 879 (2010).
- [31] M. Tillmann, B. Dakić, R. Heilmann, S. Nolte, A. Szameit, and P. Walther, *Nat. Photon.* **7**, 540 (2013).
- [32] M. Gräfe, R. Heilmann, A. Perez-Leija, R. Keil, F. Dreisow, M. Heinrich, H. Moya-Cessa, S. Nolte, D. N. Christodoulides, and A. Szameit, *Nat. Photon.* **8**, 791 (2014).